LUMINESCENCE PROPERTIES OF EUROPIUM AND TERBIUM DOUBLY ACTIVATED YTTRIUM NIOBIUM/TANTALATE PHOSPHORS UNDER X-RAY EXCITATION

M. Nazarov[1, 2], I. Arellano[1], D.Y. Noh[1], C.C. Byeon[3]

[1]Department of Materials Science and Engineering, Gwangju Institute of Science and Technology, 1, Oryong-dong, Buk-gu, 500-712, Gwangju, Republic of Korea
[2]Institute of Electronic Engineering and Industrial Technologies, Academy of Sciences of Moldova, 3/3, Academiei str., MD-2028, Chisinau, Republic of Moldova
[3]Advanced Photonics Research Institute, Gwangju Institute of Science and Technology, 1, Oryong-dong, Buk-gu, 500-712, Gwangju, Republic of Korea
(Received 23 September 2008)

Abstract

Yttrium tantalate, yttrium niobium-tantalate, and yttrium niobate doubly doped by Eu^{3+} and Tb^{3+} were investigated using X-ray diffraction and X-ray excitation luminescence in order to study their structural and luminescent properties. By means of X-ray diffraction, the crystallographic data for $YTaO_4$, $Y(TaNb)O_4$, and $YNbO_4$ with double activation by Eu^{3+} and Tb^{3+} was first calculated. Under X-ray excitation luminescence, the rare earth emission centers can contribute to the overall luminescence. The simultaneous incorporation of Eu^{3+} and Tb^{3+} ions could permit us to obtain different luminescence colors on the entire visible spectrum. Due to their various luminescence chromaticities, the proposed rare earth activated phosphors are promising materials for optoelectronics as well as for X-ray intensifying screens for medical diagnosis providing the broad variation of photoluminescence colors from blue-to-green to yellow-to-red.

1. Introduction

X-ray phosphors are materials that emit light when excited with X-rays. It may also be stimulated with lower energy sources, such as electrons or photons of ultraviolet light. Yttrium tantalate ($YTaO_4$) and yttrium niobate ($YNbO_4$) are efficient X-ray phosphors used in X-ray medical imaging, in which these phosphors are used in films/screen cassettes, and also in detectors used in electronic systems, such as computed radiography, computed tomography and fluoroscopy [1-4]. Performances of these phosphors are correlated with composition, crystalline structure, particle dimensions, and luminescence properties of powders.

In $Y(Ta,Nb)O_4$ phosphors under X-ray excitation, the blue light emission is associated with TaO_4^{3-} and NbO_4^{3-} groups from the host crystalline lattice [5]. Such luminescent emission could be shifted toward longer wavelengths when rare earth ions, such as Eu^{3+} or Tb^{3+} are used to partially replace the yttrium ions in the host crystalline lattice. In this case, Eu^{3+} and Tb^{3+} emission centers are created and can generate the corresponding red and green luminescence, respectively. The general luminescence of Eu^{3+} or Tb^{3+} in tantalates and niobates has been reported previously [1, 2, 5-7]. However, as we know, no work has been reported using doubly activated $Y(Ta,Nb)O_4$ phosphors. In this paper, we calculate the crystallographic data for $Y(Ta,Nb)O_4$ phosphors doubly activated by Eu^{3+} and Tb^{3+} using X-ray diffraction, and also study the luminescence properties of these phosphors by X-ray excitation luminescence. The X-ray luminescence is compared with PL spectra.

2. Experimental procedures

2.1. Sample preparation

Yttrium tantalate ($YTaO_4$), yttrium niobium-tantalate ($YTaNbO_4$), and yttrium niobate ($YNbO_4$) phosphors activated by the rare earth elements, such as Eu^{3+} and Tb^{3+}, were prepared by solid state reaction from homogeneous mixture consisting of Y_2O_3 (99.9%), Ta_2O_5 (Optipur), and Nb_2O_5 (99%). The oxide precursors for the host lattice, Eu_2O_3 and/or T_4O_7, are used in the activator system under the flow of Na_2SO_4 (99%). The mixtures were homogenized with a ball mill, in acetone medium, and dried at 70°C. The phosphor samples were baked at 1200°C for 4 h and slowly cooled to room temperature. Finally, the samples were water washed, dried, and sieved.

2.2. X-ray studies

2.2.1. X-ray diffraction measurement. The crystal structures of the prepared samples were investigated using a Rigaku X-ray diffractometer with Cu-Kα (λ=1.5418 Å) line and an anode operating at 40 kV and 40 mA. The scan speed was 2 s per step (0.02º step-2θ) while covering the range between 10º and 80º.

2.2.2. X-ray luminescent measurement. To study phosphor luminescence under X-ray excitation, a Rigaku X-ray diffractometer with an anode operating in the range from 20 to 50 kV and 100 mA was used. The experimental configuration is illustrated in Fig. 1.

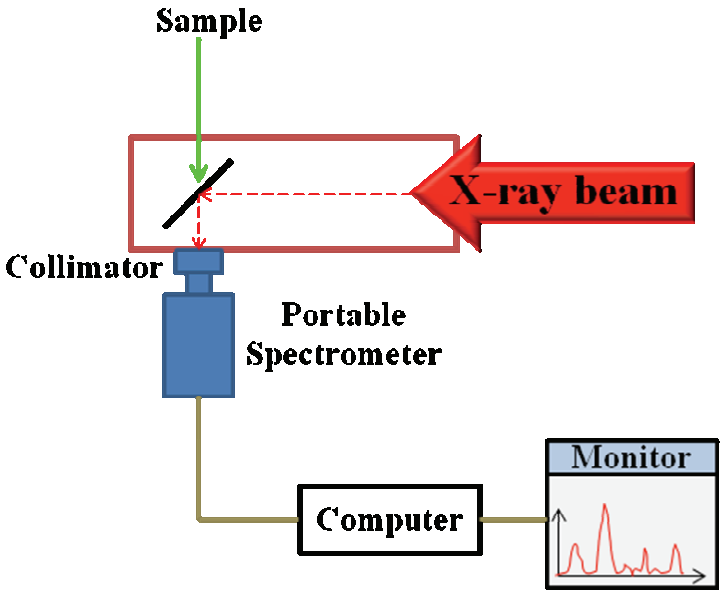

Fig. 1. Experimental set-up to study the luminescence of phosphors under X-ray excitation.

As broadband X-ray radiation hits the sample, some of the luminescence is collected by a collimator system. The emission spectrum is recorded with a portable spectrometer (SM240, Spectral Products) with 200 ~1200 nm detection range.

Three types of host lattices with double activation by rare earth elements Eu^{3+} and Tb^{3+} were prepared. General formula of phosphors is $Y_{1-x-y}Eu_xTb_yTa_{1-z}Nb_zO_4$. We used in our experiments x = 0.025, y = 0.025, and z = 0, 0.15, or 1. The phosphor compositions of prepared samples are listed in Table 1.

Table 1. Composition of yttrium tantalite/niobate phosphors with double activation by Eu^{3+} and Tb^{3+}.

N	Phosphor type	Phosphor formula	Host lattice (mol%)		Re-activator (mol%)	
			$YTaO_4$	$YNbO_4$	Eu^{3+}	Tb^{3+}
1	$YTaO_4$:Eu,Tb	$Y_{0.95}Eu_{0.025}Tb_{0.025}TaO_4$	100	-	2.5	2.5
2	$Y(TaNb)O_4$:Eu,Tb	$Y_{0.95}Eu_{0.025}Tb_{0.025}Ta_{0.85}Nb_{0.15}O_4$	85	15	2.5	2.5
3	$YNbO_4$:Eu,Tb	$Y_{0.95}Eu_{0.025}Tb_{0.025}NbO_4$	-	100	2.5	2.5

3. Results and discussion

3.1. X-ray Diffraction characterization

In Fig. 2, we show the X-ray diffraction (XRD) spectra of three different host lattices: a) $YTaO_4$, b) $YNbO_4$, and c) $Y(TaNb)O_4$ with double activation.

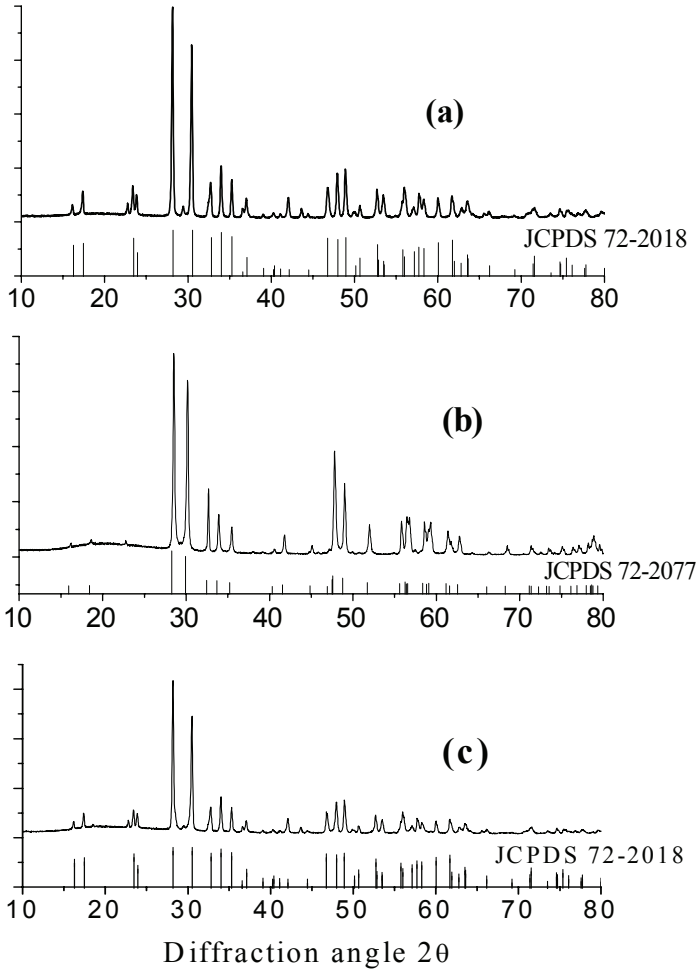

Fig. 2. XRD patterns of (a) $YTaO_4:Eu^{3+},Tb^{3+}$, (b) $YNbO_4:Eu^{3+},Tb^{3+}$, (c) $Y(Ta,Nb)O_4:Eu^{3+},Tb^{3+}$.

a) $YTaO_4$ has generally three crystal structures; scheelite (tetragonal, T), fergusonite (monoclinic, M), and another monoclinic form, called M' [2, 8]. The crystal structure depends on synthesis conditions and temperature. M' structure presents more efficient charge transfer process that provides superior luminescent emission. It is the M' modification that is used in phosphor screens. Our $YTaO_4:Eu^{3+},Tb^{3+}$ phosphors (Fig. 2a) show M'- $YTaO_4$ crystal structure.

b) Contrary to the $YTaO_4$, which exhibits three structures, the $YNbO_4$ structure exhibits only one structural type (fergusonite). X-ray diffraction spectrum of $YNbO_4:Eu^{3+},Tb^{3+}$ (Fig. 2b) shows the evidence of the monoclinic M-$YNbO_4$ fergusonite crystal structure.

c) Partial substitution of the tantalum ions by 15% mole niobium ions in the system $Y(TaNb)O_4:Eu^{3+},Tb^{3+}$ did not change the M' crystal structure of $YTaO_4$. This conclusion is also confirmed in other works [9, 10].

We also found that the incorporation of the rare earth ions into M'-$YTaO_4$ structure and into M-$YNbO_4$ structure did not change the basic structure significantly, but increased the unit cell volume according to the Vegard's law. The amounts of the unit cell volume increment were 0.229% for $YTaO_4:Eu^{3+},Tb^{3+}$ and 0.153% for $YNbO_4:Eu^{3+},Tb^{3+}$ over the volume of the original host lattices. The difference in the ionic radii of yttrium, terbium, and europium (1.16 Å, 1.18 Å, and 1.20 Å, respectively) may account for these increments.

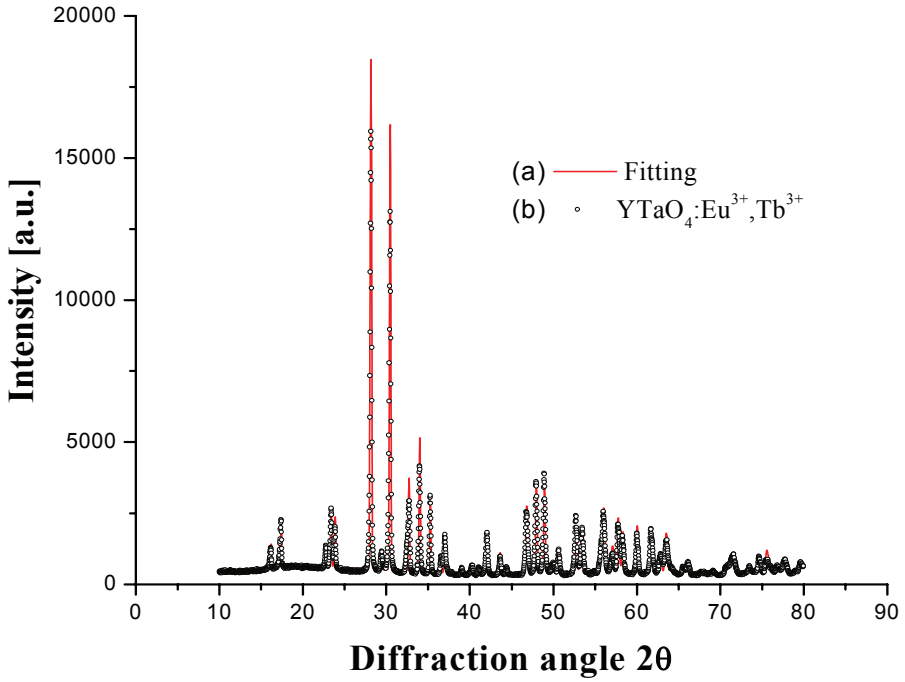

Fig. 3. XRD patterns of $YTaO_4:Eu^{3+},Tb^{3+}$ and it Rietveld fitting.

Figure 3 shows the X-ray diffraction patterns of the $YTaO_4:Eu^{3+},Tb^{3+}$ phosphor. Its spectral peak positions are in a good agreement with Rietveld fitting (Fig. 3a) and also the data given in Powder Diffraction File JCPDS 72-2018 International Center for Diffraction (Fig. 2a). The black points in Fig. 3b are the measured data and the solid line (a) is the calculation result of the Rietveld analysis, which was developed by Rietveld for structure profile refinement of X-ray powder diffraction data [11]. The Rietveld calculation provides the crystallographic information by comparing the model profile with X-ray or neutron curves using the method of least squares. One uses the Rietveld analysis generally to get the lattice parameters, atomic positions, and atomic distances. The peak positions of X-ray diffraction curve are related to the unit cell lattice constants of the crystal structure; the peak intensities are affected by various parameters, such as atomic position, atomic occupancy, and thermal effect. No work has been published using Rietveld analysis for these phosphors doubly activated. We applied the Rietveld analysis for all investigated phosphors. The detailed crystallographic information of the measured phosphors from the Rietveld analysis is listed in Table 2 and Table 3. From the occupation factor *F* (Table 2), one can see that $F = 1$, which means the site is fully occupied by an atom.

Table 2. Atomic positions and lattice parameters for different host lattices.

M'-$YTaO_4$:Eu^{3+},Tb^{3+}	*Atom*	*x*	*y*	*z*	*F*
a=5.298Å	Y	0.25	0.7605	0	1
b=5.461Å	Ta	0.25	0.3111	0.5	1
c=5.112Å	O(1)	0.4192	0.4033	0.3079	1
β=96.37	O(2)	0.1230	0.1117	0.2824	1
M'-Y(TaNb)O_4:Eu^{3+},Tb^{3+}	*Atom*	*x*	*y*	*z*	*F*
a=5.299Å	Y	0.25	0.726	0	1
b=5.476Å	Ta	0.25	0.2611	0.5	1
c=5.072Å	O(1)	0.5251	0.4236	0.2746	1
β=94.51	O(2)	0.0857	0.0810	0.2140	1
M-$YNbO_4$:Eu^{3+},Tb^{3+}	*Atom*	*x*	*y*	*z*	*F*
a=7.617Å	Y	0	0.3791	0.25	1
b=10.95Å	Nb	0	0.8551	0.25	1
c=5.298Å	O(1)	0.2286	0.79	0.2422	1
β=138.42	O(2)	0.2519	0.9576	0.6818	1

Table 3. Interatomic distances between anions and cations of different host lattices.

Structure	*Y-O (Å)*	*Ta-O (Å)*	*Nb-O (Å)*
M'-$YTaO_4$:Eu^{3+},Tb^{3+}	O(1) 2x 2.602 O(2) 2x 2.536 O(1) 2x 2.639 O(2) 2x 2.417	O(1) 2x 1.489 O(1) 2x 2.467 O(2) 2x 1.646	
M'-Y(TaNb)O_4:Eu^{3+},Tb^{3+}	O(1) 2x 2.548 O(2) 2x 2.422 O(1) 2x 2.074 O(2) 2x 2.271	O(1) 2x 2.124 O(1) 2x 2.344 O(2) 2x 1.907	
M-$YNbO_4$:Eu^{3+},Tb^{3+}	O(1) 2x 2.543 O(2) 2x 2.205 O(1) 2x 2.258 O(2) 2x 2.423		O(1) 2x 1.911 O(1) 2x 2.391 O(2) 2x 1.900

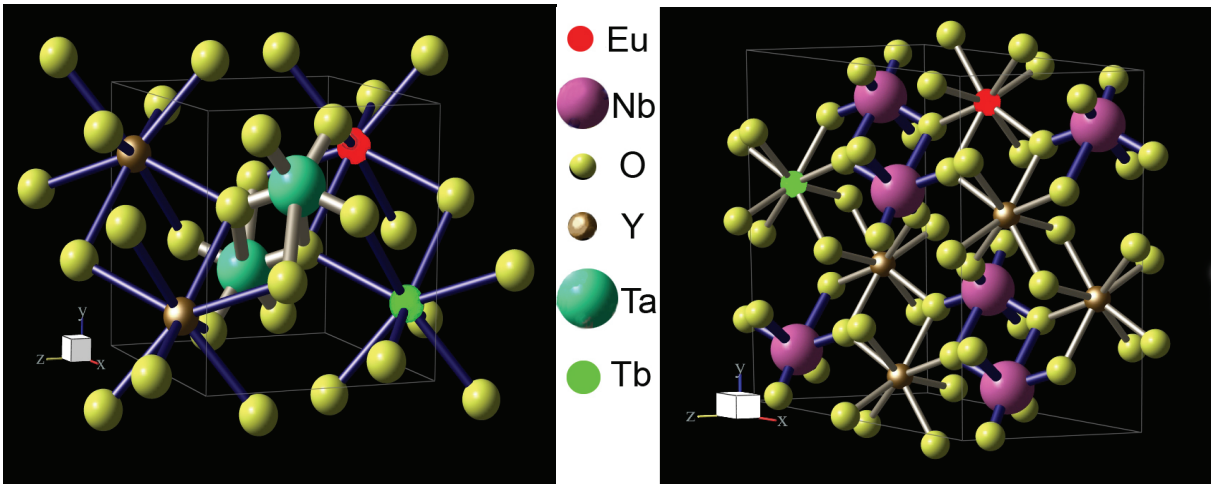

Fig. 4. Crystal structure of (a) M'-$YTaO_4$ and (b) M-$YNbO_4$ with double activation by Eu^{3+} and Tb^{3+}.

Using the data in Table 2 and Table 3 the structures M'-$YTaO_4$ and M-$YNbO_4$ with double activation by Eu^{3+} and Tb^{3+} were calculated. Figure 4 illustrates the process of rare earth activators Eu^{3+} and Tb^{3+} substituting yttrium atoms from the host lattice.

In M'-$YTaO_4$:Eu^{3+},Tb^{3+}, the Y atoms (Fig. 4a) are surrounded by 8-coordinated oxygen atoms forming a distorted cube [9]. The Y-O average distance is 2.548 Å. The Ta atoms (Fig. 4a) are in a distorted octahedral coordination with four shorter Ta-O bonds at 1.489 Å and 1.646 Å and two longer at 2.467 Å. The total amount of atoms inside of the M'-$YTaO_4$ structure is the following: 2 yttrium atoms, 2 tantalum, and 8 oxygen atoms, which is the same as that reported previously [12].

Following the same procedure, we calculated and drew the crystallographic structure of $YNbO_4$:Eu^{3+},Tb^{3+}. The Y atoms are also surrounding by 8-coordinated oxygen atoms forming a distorted cube. The Y-O average distance is 2.357 Å. The Ta atoms are in a distorted octahedral coordination, with four shorter Nb-O at 1.900 Å and 1.911 Å and two longer at 2.391 Å. The total amount of atoms inside of the M-$YNbO_4$ structure is the following: 4 yttrium atoms, 4 tantalum atoms, and 16 oxygen atoms.

As we have shown in Fig. 2, the incorporation of the rare earth ions to M'-$YTaO_4$ structure and to M-$YNbO_4$ structure does not change significantly the basic structure and the results do not differ from those reported before. However, as we will see, the incorporation of rare earth ions to the host lattices may change the luminescent properties of the investigated phosphors.

3.2. X-ray luminescence characterization

The X-ray luminescence spectra were measured as shown in Fig. 1. The measurement of X-ray luminescence was performed with X-rays generated from a Rigaku rotating anode operating at 5 kW. Figure 5 depicts the luminescence spectra of M'-$Y(Ta,Nb)O_4$ and M-$YNbO_4$ activated by Eu^{3+} and Tb^{3+} when they were exposed into the X-ray beam. We also found the linear dependence of luminescence intensity under different applied voltage in the range from 20 to 50 kV.

When rare earth ions, such as Eu^{3+} and Tb^{3+}, are used simultaneously to partially substitute the yttrium ions from the host crystalline lattice, Eu^{3+} and Tb^{3+} emission centers are created. In this case, the luminescence can be red-shifted toward longer wavelengths, and both emission centers can contribute to the overall luminescence. The emission spectra were measured in the range from 200 to 1200 nm, but the main peaks were found in the range from 450 to 725 nm. In Fig. 5 the first 2 peaks at 490 nm ($^5D_4 \rightarrow {}^7F_6$) and at 545 nm ($^5D_4 \rightarrow {}^7F_5$) correspond to terbium, and the peaks at 590 nm ($^5D_0 \rightarrow {}^7F_1$), 612 nm ($^5D_0 \rightarrow {}^7F_2$), and 705 nm ($^5D_0 \rightarrow {}^7F_4$) are the europium contribution to the luminescence. The doubly activated M'-$YTaO_4$ structure shows the better luminescence compared with M-$YNbO_4$. The incorporation of these 2 activators into the host crystalline lattice substituting the yttrium ions seems to efficiently enhance the charge-transfer process for the M'-$YTaO_4$ structure, where the average Ta-O distances are smaller in M' structure than Nb-O distances in M structure. Under X-ray excitation, it is quite reasonable to assume that the excitation energy is absorbed first by the host lattice, which involves the transition between 4d-like states of Y and 2p-like states of O [13]. The absorbed energy may then be transferred to TaO_4^{-3} and NbO_4^{-3} groups and at last transferred to the Eu^{3+} and Tb^{3+} emission centers. It is also possible that, in certain energy conditions, a process of energy transfer appears between activators, because of the proximity of the $^5D_4$ (Tb^{3+}) and $^5D_1$ (Eu^{3+}) energy levels [14]. In this case, the Eu–Tb activator couple could work as donor–acceptor pair.

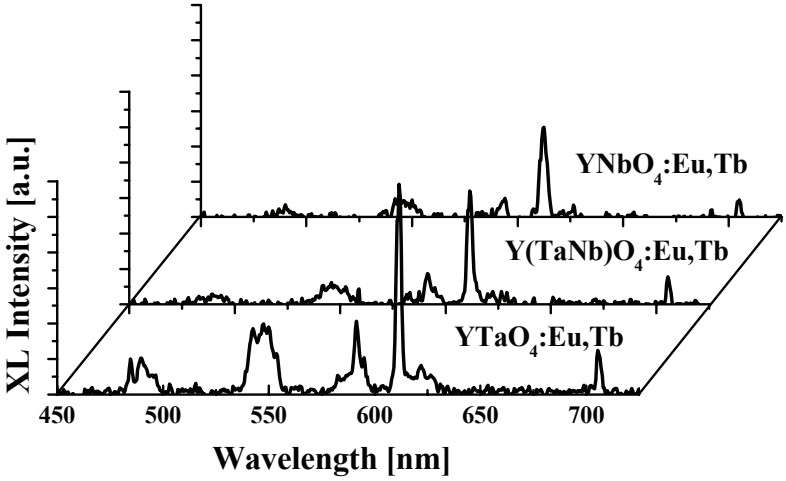

Fig. 5. X-ray emission spectra of different host lattices with double activation by Eu^{3+} and Tb^{3+}, U=50 kV.

The luminescence intensities of Tb^{3+} and especially of Eu^{3+} under X-ray excitation were much higher in comparison with UV excitation. Moreover, the strong Eu^{3+} emission of $^5D_0 \rightarrow {}^7F_4$ appears at 705 nm. Usually this emission is very weak and could not be seen under UV excitation [15]. PL measurement was carried out and we found that the branch ratio, comparing the relative intensity of $^5D_0 \rightarrow {}^7F_j$ emission peaks under UV (254 nm) and X-ray excitation (50 kV, 100 mA), varies with not only the host lattices but also with the incorporation of the rare earth activators and the activation excitation wavelength. The detailed branching ratios of $^5D_0 \rightarrow {}^7F_j$ transitions are presented in Table 4.

Table 4. Branching ratios of $^5D_0 \rightarrow {}^7F_j$ transitions (Eu^{3+} and Tb^{3+} concentration = 5 mol %).

Transitions	$YTaO_4:Eu^{3+},Tb^{3+}$		$Y(TaNb)O_4:Eu^{3+}, Tb^{3+}$		$YNbO_4:Eu^{3+}, Tb^{3+}$	
	UV	X-ray	UV	X-ray	UV	X-ray
$^5D_0 \rightarrow {}^7F_1$	48	30	39	26	25	13
$^5D_0 \rightarrow {}^7F_2$	100	100	100	100	100	100
$^5D_0 \rightarrow {}^7F_4$	1.3	25	1.4	22	1.1	13

Under UV excitation the $^5D_0 \rightarrow {}^7F_4$ emission is mostly trapped by the empty upper levels. In contrast to the UV excitation, it is more likely that such empty levels can be readily filled under X-ray excitation. High-energy photons of X-ray excitation are absorbed in the conduction band of the sample creating charge carriers like free electrons in the conduction band and holes in the valence band. In other words, excitation in the X-ray range produces electron–hole pairs that undergo recombination at activator ions and fill the traps. This model explains the appearance of visible $^5D_0 \rightarrow {}^7F_4$ transition and the increment of the luminescence intensity of Eu^{3+} and Tb^{3+} emission centers under X-ray excitation.

4. Conclusions

The structures $Y(Ta,Nb)O_4$ with double activation by Eu^{3+} and Tb^{3+} were studied and the crystallographic data for these phosphors were calculated. The activator incorporation was estimated by XRD. We found that the addition of the rare earth ions does not change the basic structure, but increases the luminescence. Under X-ray excitation, the doubly activated

$YTaO_4:Eu^{3+},Tb^{3+}$ shows the best luminescence intensity compared to $YNbO_4$: Eu^{3+},Tb^{3+} and $Y(TaNb)O_4:Eu^{3+},Tb^{3+}$. These phosphors may be applied to the X-ray intensifying screens for medical diagnosis providing various photoluminescence colors.

Acknowledgments

This work was supported by BK21 Program funded by the Ministry of Science and Technology of Korean government, and by the Korean Science and Engineering Foundation (KOSEF) through National Research Laboratory (Program No. M10400000045-04J0000-04510). The authors thank also Elisabeth-Jeanne Popovici (”Raluca Ripan” Institute for Research in Chemistry, Babes Bolyai University, 30, Fantanele str., 400294, Cluj-Napoca, Romania) for sample preparation.

References

[1] G. Blasse and B.C. Grabmaier, Luminescent Materials, Springer Verlag, Berlin, 232, 1994.
[2] L.H. Brixner, Mater. Chem. Phys., 16, 253, (1987).
[3] M. Sonoda, M. Takano, J. Miyahara, and H. Kato, Radiology, 148, 833, (1983).
[4] C.D. Greskovich, D. Cusano, D. Hoffman and R.J. Riedner, Amer. Ceram. Soc. Bull., 71, 1120, (1992).
[5] G. Blasse and A. Bril, J. Electrochem Soc., 115, 10, 1067, (1968).
[6] G. Blasse and A. Bril, J. of Lumin., 3, 109, (1970).
[7] A. Bril, W.L. Wanmaker, and R.E. Schuil, in: Intern. Symp. on Luminescence, Munich, 310, (1965).
[8] G.M. Wolten, The structure of the M’-phase of $YTaO_4$, a third fergusonite polymorph, Acta Crystallogr., 23, 939, (1967).
[9] L.H. Brixner and H. Chen, J. Electrochem. Soc., 130, 2435, (1983).
[10] A. Hristea, E.J. Popovici, L. Muresan, M. Stefan, R. Grecu, A. Johansson, and M. Boman, J. Alloys and comp., (2008), (in press).
[11] H.M. Rietveld, Acta Cryst., 22, 151, (1967).
[12] S.L. Issler, C.C. Torardi, J. Alloy. Compd., 229, 1, 54, (1995).
[13] K.S. Sohn, W. Zeon, H. Chang, S.K. Lee, and H.D. Park., Chem. Mater., 14, 2140, (2002).
[14] M.V. Nazarov, D.Y. Jeon, J.H. Kang, E.J. Popovici, L-E. Muresan, M.V. Zamoryanskaya, and B.S. Tsukerblat, Solid State Commun., 131, 307, (2004).
[15] E.J. Popovici, M. Nazarov, F.I. Lucaci, D.Y. Noh, M. Stefan, and E. Indrea, Proc. of the 15th Int. conf. on luminescence and optical spectroscopy of condensed matter, ICL-08, Lyon, July 7-11, France, 219, (2008).